Electron-scattering cross sections for selected alkyne molecules: Measurements and calculations

Czesław Szmytkowski,* Paweł Możejko, Mateusz Zawadzki, Krzysztof Maciąg, and Elżbieta Ptasińska-Denga
Atomic Physics Division, Department of Atomic, Molecular and Optical Physics, Faculty of Applied Physics and Mathematics, Gdańsk University of Technology, ul G. Narutowicza 11/12, 80-233 Gdańsk, Poland
(Received 27 March 2014; published 7 May 2014)

We report cross-section results from experimental and theoretical studies on electron collisions with 1-butyne ($HC{\equiv}C–CH_2CH_3$) and acetylene ($HC{\equiv}CH$) molecules and from computations for a propyne ($HC{\equiv}C–CH_3$) molecule. Absolute *grand* -total electron-scattering cross sections (TCSs) were measured at impact energies ranging from about 0.5 to 300 eV using the linear electron-transmission method. The TCS energy curve for 1-butyne has a very broad enhancement on which some distinct features are superimposed, namely a resonant-like maximum (located near 3.2 eV), a broad hump (centered around 7.5 eV), and a shoulder (spanned between 12 and 26 eV). The shape of our experimental TCS curve for acetylene closely resembles that reported earlier, while its magnitude is usually larger. As no previous calculations for electron collisions with 1-butyne and propyne are disclosed in the literature, we computed the elastic (ECS) and ionization (ICS) cross sections for these molecules. Similar calculations were also performed for acetylene molecules. The additivity rule was employed to calculate the ECSs from 50 to 3000 eV, while the binary-encounter-Bethe approach was used for computation of the ICSs, from the threshold up to 3000 eV. The sum (ECS + ICS) of these two computed cross sections reasonably reproduces the TCS measurements above 50 eV. Furthermore, the experimental TCS curves, obtained in our laboratory, for a series of acetylenic compounds—acetylene ($HC{\equiv}CH$), propyne ($HC{\equiv}C–CH_3$), and 1-butyne ($HC{\equiv}C–CH_2CH_3$)—are compared to study the substitutional effect. Finally, the influence of the structural differences on the electron-scattering TCS for isomers of the C_4H_6 molecule (1-butyne, 2-butyne, and 1,3–butadiene) is indicated and discussed.

DOI: 10.1103/PhysRevA.89.052702 PACS number(s): 34.80.Bm, 34.80.Gs

I. INTRODUCTION

The study of electron scattering from molecules plays an important role in the understanding of the electron-driven physicochemical phenomena in various environments, such as biological media [1], planetary atmospheres, interstellar clouds [2], and plasmas [3–5]. Therefore, when modeling and simulating effects induced by electrons traversing through matter, the comprehensive set of reliable electron-scattering cross sections and electron transport coefficients for a variety of compounds, including hydrocarbon molecules, is necessary as input data.

Studies on the electron-assisted processes involving 1-butyne molecules started some decades ago; however, the electron-scattering results available in the literature are scarce and fragmentary. Early electron-impact experiments for 1-butyne were devoted to the determination of the appearance potentials of ions and bond energies [6,7]. Later, the excitation spectra over the subionization energy range were obtained by means of a trapped-electron technique [8,9]. More attention was dedicated to electronic excitation of 1-butyne molecules by electron impact at energies above the ionization threshold [10–12]. One would also note a study employing a gas electron diffraction technique, in which the geometrical structure of a 1-butyne molecule was determined [13]. The only absolute electron-scattering intensities restrain to cross sections for the electron attachment with negative ion formation [14], at electron incident energies below 15 eV. To our knowledge, no absolute total cross sections (TCSs), either measured or calculated, have been reported yet for electron scattering by 1-butyne molecules.

For acetylene, contrary to more complex hydrocarbon molecules, there is quite a large number of the electron-scattering TCS results, both experimental [15–21] and theoretical [22–28]. Early absolute TCS measurements, carried out more than 80 years ago [15,16], cover energies below 50 eV, while recent absolute TCS data concern rather high electron-impact energies [17–19], above 200 eV. It is worth noting that between 50 and 200 eV, the only available experimental TCS values were those normalized ones [21]. Theoretical TCS results from various research groups [22–25,27,28] differ from each other with regard to the magnitude even by a factor of 2, in the energy range from 50 to 1000 eV. These differences motivated the present calculations for acetylene. A more comprehensive summary of theoretical and experimental investigations on electron-acetylene molecule collisions over a very wide energy range is available in Refs. [28,29].

One of the goals of the present work is to provide reliable absolute experimental TCS data for 1-butyne over a wide electron-impact energy range, from about 1 to 300 eV. For the TCS measurements, the linear electron-transmission method has been employed. To extend the electron-scattering data to higher energies, beyond the range of our experiment, we computed TCS=ECS + ICS values based on our elastic (ECS) and ionization (ICS) cross-section calculations. Moreover, the TCS values for 1-butyne, derived from empirical formulas [19,30], are also presented with the intention of testing their applicability. As 1-butyne is a substituted homologue of acetylene, it is also interesting to examine how replacing one hydrogen atom in an acetylene molecule with various atomic groups changes the electron-molecule scattering dynamics. For a demonstration of the substitutional effect, we use the experimental absolute TCS data for acetylene ($HC{\equiv}CH$),

*czsz@mif.pg.gda.pl

propyne ($HC{\equiv}C–CH_3$) [31], and 1-butyne ($HC{\equiv}C–CH_2CH_3$). As for a proper comparison, it is more appropriate to have data from the same laboratory; the TCS for $HC{\equiv}CH$ was also measured in the present work. Additionally, our measurements fill the gap of the 50–200 eV electron-acetylene TCS absolute data available in the literature. Moreover, the experimental TCS results for substituted acetylenes are complemented with the sum, ECS + ICS, of the integral elastic and ionization cross sections, which we have calculated up to 3000 eV for acetylene, propyne, and 1-butyne. To investigate how the arrangement of atoms in the target molecule is reflected in the shape and magnitude of the TCS energy dependence, we compared the present experimental TCS results for 1-butyne with our earlier measured TCSs for 2-butyne and 1,3-butadiene [32], other isomers of the C_4H_6 compound.

II. MEASUREMENTS

The present measurements of the TCSs for the electron-molecule collision were carried out in linear electron-transmission mode using the electron spectrometer extensively employed in a series of recent TCS experiments performed in our laboratory. Details of the experimental arrangement and procedure have already been described in detail elsewhere [33], thus only a brief summary is given below.

A low-energy primary electron beam is generated with a hot filament and is formed by an assembly of electrostatic lenses followed by an energy-dispersing 127° electrostatic deflector. Then, the electrons of desired energy E [$\Delta E \simeq$ 0.1 eV, full width at half-maximum (FWHM)] are directed into the reaction cell, where projectiles may interact with the target particles under study. The electrons, which leave the scattering cell through the exit orifice, are discriminated against energy with the retarding field lens stack and eventually collected with the Faraday cup. To assure that the trajectories of the unscattered electrons are straight lines within the interaction and detection regions, the residual magnetic field along the whole electron pathway in the spectrometer is reduced below 100 nT. The electron optics is housed in a vacuum chamber pumped to the background pressure of about 20 μPa.

In the electron-transmission method, the TCS at a given electron impact energy, E, is determined based on the Bouguer–de Beer–Lambert (BBL) attenuation formula,

$$\mathrm{TCS}(E) = \frac{k\sqrt{T_t T_m}}{p\,L} \ln \frac{I_0(E)}{I_p(E)},$$

where $I_p(E)$ and $I_0(E)$ are the measured intensities of the electron beam passing through the reaction cell in the presence or absence of the target gas, respectively, L is the length of the effective electron pathway within the target, and k is the Boltzmann constant. In the present experiment, the temperature of the target cell, T_t, measured with a microsensor, appeared to be lower by about 5–25 K from that of the MKS capacitance head, $T_m = 322$ K. Therefore, the measured target pressure p was corrected to account for the thermal transpiration effect [34].

The acquisition of data, necessary for the TCS derivation, and their processing were controlled by a computer. As the quantities in the BBL formula are taken directly in the present experiment, the TCS values reported in this work are given in absolute units, without any normalization procedure. The final TCS at given energy E is the weighted average of a number of TCS values obtained at a range of target pressures and different electron optics conditions. The TCS uncertainties of the random nature, estimated as one standard deviation of the weighted mean value, are well below 1%, between 2 and 100 eV, and do not exceed 2% over the whole remaining range of the electron-impact energies applied. However, due to instabilities of the electron current at energies below 0.5 eV, the statistical uncertainty of the TCS at the lowest energies applied amounts of about 5%.

It is worthwhile to emphasize that despite the simplicity of the idea of TCS measurements with the electron-transmission technique, tens years of its usage, and declared care in experiments, considerable divergences among TCS values, coming from different laboratories, were noticed [35]. These differences are related to many factors, which may systematically overcharge the measurements of particular quantities necessary for the TCS determination [36]. Below we single out those effects that may permanently distort the TCS data obtained in the present experiment.

A significant unavoidable error in the electron-transmission method is connected with the fact that the detector assembly does not distinguish electrons scattered elastically into small forward angles from those not scattered. Due to this *forward-scattering effect*, the measured intensity of the transmitted electron current, $I_p(E)$, is somewhat overestimated, leading to systematic lowering of the measured TCS with respect to its *exact* value. The analysis of the discrimination ability of the electron optics against elastically scattered electrons shows that the forward-scattering effect can lead to significant changes in the magnitude of the measured TCS, and, as shown recently by Sullivan *et al.* [37], also in the shape of the TCS energy dependence, especially at low electron-impact energies. Applying the appropriate differential cross-section data and taking into account the geometry of the scattering and detection regions, one can roughly estimate how the forward scattering influences the measured TCS. We have found that the inability to discriminate electrons scattered elastically through the small angles in the forward direction may lower our measured TCSs between 5 and 50 eV by about 2%, and below 2 eV the TCS lowering may increase to 4–6%. The TCS data reported in this work are not corrected for the forward-scattering effect.

The inevitable effusion of target molecules through the scattering cell orifices leads to the inhomogeneity of the target pressure along the cell and to the presence of target particles outside the orifices; this last effect may result in a noticeable number of scattering events occurring just beyond the cell. Following the electron path-length calculations [38], we have estimated that the denominator pL in the BBL formula, taken as the product of the pressure, p, measured in the center of the cell and the geometrical distance ($L = 30.5$ mm) between entrance and exit cell apertures, may be erroneous to within 2%.

1-butyne (98.8%) and acetylene (99+%) were purchased from Chemos GmbH and Air Products and Chemicals, respectively. To allow stable experimental conditions, the target handling system was kept at elevated temperature of about 315 K. When the sample species was admitted, the pressure in the reaction cell was kept within 80–200 mPa, while the pressure in the vacuum chamber was always less than 0.2 mPa. At such working pressures, multiple scattering events were minimized and no systematic variation of the measured TCSs with the target pressure was observed.

The electron-impact energy scale can be determined against the 2.3 eV resonant structure in a molecular nitrogen with an accuracy better than 0.1 eV. However, due to contamination of the electron optics elements with the target molecules, a drift in energy up to 0.1 eV was noticed during the long-term experiment. That effect may somewhat distort the TCS structures visible at low impact energies. As the contamination gradually lowered also the intensity of the primary electron current over a period of several weeks, one or two cleanings of the electron optics were necessary during the course of the experiment.

Other possible TCS systematic errors, related to quantities taken in the experiment, are estimated to be less than 1% each. The overall systematic uncertainty of our absolute TCSs for 1-butyne, evaluated as a sum of all individual potential systematic uncertainties, amounts to up to 15%, between 0.5 and 1 eV, decreasing to 9–11% within 1–2 eV, and to about 6–7% between 2 and 100 eV, increasing again to 8–9% at higher energies. At the two lowest energies applied, 0.3 and 0.4 eV, the overall uncertainty of the respective TCS values reaches even 20%. The respective TCS systematic errors for acetylene are expected to be lower by 2–4%.

III. CALCULATIONS

To extend our studies to higher energies and to get information on the elastic and ionization scattering channels, we performed numerical calculations of the elastic and ionization cross sections using simple but reliable theoretical models. The elastic cross sections have been calculated for the 50–3000 eV electron collisions, while cross sections for electron impact ionization have been obtained for energies ranging from the ionization threshold of the studied targets up to 3 keV. Having in hand the total ECS and the ICS over a wide energy range, it was possible to estimate the total electron-scattering cross section even far beyond the range of the present experiment, as the sum of the ECS and the ICS. Because at intermediate and high energies the contribution from the ionization and elastic channels dominates the electron scattering from molecular targets, such a simple approximation yields reasonable total electron-scattering data at higher energies for quite complex molecules [39–41].

The elastic cross sections for electron scattering from molecules that are the object of the interest have been calculated with the additive rule (AR) method [42,43] at the static+polarization level of approximation, while the electron-impact ionization cross sections have been obtained within the binary-encounter-Bethe (BEB) formalism [44,45]. We provide here only a brief description of theoretical methods and computational procedures used, since they have been presented in more detail in our earlier works [46,47].

In the AR approximation, the electron-molecule collision is reduced to the problem of scattering by individual atoms, the constituents of the target molecule. In this approach, the total elastic cross section for electron scattering from molecules is given by

$$\sigma(E) = \sum_{i=1}^{N} \sigma_i^A(E),$$

where E is an energy of the incident electron. The elastic atomic cross section for the ith atom of the target molecule, $\sigma_i^A(E)$, has been derived according to

$$\sigma^A = \frac{4\pi}{k^2}\left(\sum_{l=0}^{l_{\max}}(2l+1)\sin^2\delta_l + \sum_{l=l_{\max}}^{\infty}(2l+1)\sin^2\delta_l^{(B)}\right),$$

where $k = \sqrt{2E}$ is the wave number of the incident electron; note that in this section, atomic units are used.

To obtain phase shifts, δ_l, the radial Schrödinger equation

$$\left[\frac{d^2}{dr^2} - \frac{l(l+1)}{r^2} - 2[V_{\text{stat}}(r) + V_{\text{polar}}(r)] + k^2\right] u_l(r) = 0$$

has been solved numerically under the boundary conditions

$$u_l(0) = 0, \quad u_l(r) \overset{r\to\infty}{\longrightarrow} A_l \hat{j}_l(kr) - B_l \hat{n}_l(kr),$$

where $\hat{j}_l(kr)$ and $\hat{n}_l(kr)$ are the Riccati-Bessel and Riccati-Neumann functions, respectively. The phase shifts are connected with the asymptotic form of the wave function, $u_l(r)$, by

$$\tan\delta_l = \frac{B_l}{A_l}.$$

As in our earlier studies, in the present work the electron-atom interaction has been described as static polarization only with the static, $V_{\text{stat}}(r)$ [48], plus polarization, $V_{\text{polar}}(r)$ [49], model potentials. The respective potentials are given by the following expressions:

$$V_{\text{stat}}(r) = -\frac{Z}{r}\sum_{m=1}^{3} A_m \exp(-\beta_m r),$$

where Z is the nuclear charge of the atom, and A_m and β_m are parameters obtained by the fitting procedure to the numerical Dirac-Hartree-Fock-Slater screening function [48],

$$V_{\text{polar}}(r) = \begin{cases} \nu(r), & r \leqslant r_c, \\ -\alpha/2r^4, & r > r_c, \end{cases}$$

where $\nu(r)$ is the free-electron-gas correlation energy [50], α is the static electric dipole polarizability of the atom, and r_c is the first crossing point of the $\nu(r)$ and $-\alpha/2r^4$ curves [51].

According to the BEB model [44,45], the electron-impact ionization cross section per molecular orbital is given by

$$\sigma^{\text{BEB}} = \frac{S}{t+u+1}\left[\frac{\ln t}{2}\left(1-\frac{1}{t^2}\right) + 1 - \frac{1}{t} - \frac{\ln t}{t+1}\right],$$

where $u = U/B$, $t = T/B$, $S = 4\pi a_0^2 N R^2/B^2$, $a_0 = 0.5292$ Å, $R = 13.61$ eV, and T is the energy of the impinging electron. Finally, the total cross section, σ^{ion}, for electron-impact ionization of a molecule can be obtained as the sum of the ionization cross sections for all molecular orbitals,

$$\sigma^{\text{ion}} = \sum_{i=1}^{n_{\text{MO}}} \sigma_i^{\text{BEB}},$$

where n_{MO} is the number of the given molecular orbital, B is the electron binding energy, U represents the kinetic energy of the orbital, and N is the orbital occupation number. At first, all studied molecules have been geometrically optimized within proper symmetry. Then, the electron binding energies and their kinetic energies have been calculated with the Hartree-Fock (HF) method using the GAUSSIAN code [52] and the GAUSSIAN 6-31 G basis set. Obtained in this way, ionization energies are not precise enough and usually can differ from experimental ones by about 1–2 eV. Therefore, it was necessary to perform the outer valence Green function (OVGF) calculations of ionization potentials [53–56] using the GAUSSIAN.

IV. RESULTS AND DISCUSSION

In this section, we present our experimental and theoretical results for the electron scattering from 1-butyne and acetylene, while for the propyne molecule only the calculations are executed. The absolute *grand* -total electron-scattering cross sections were measured in the linear electron-transmission experiments, over the energy range from 0.3 to 300 eV for 1-butyne and within 0.6–270 eV for acetylene molecules. The integral ECS and ICS were computed, both up to 3 keV, in the additivity rule approximation and the BEB approach, respectively. The sum of the ECS and ICS is then compared with the measured TCS. Thereafter, we compare TCSs for the family of homologous compounds—acetylene (HC≡CH), propyne (HC≡C–CH_3), and 1-butyne (HC≡C–CH_2CH_3)—to determine if the replacement of one hydrogen atom in the acetylene with different functional groups changes the respective TCS energy dependences. Furthermore, we compare the absolute experimental TCSs for three isomers of the C_4H_6 compound—1-butyne (HC≡C–CH_2CH_3), 2-butyne (H_3C–C≡C–CH_3), and 1,3 butadiene (H_2C=CHCH=CH_2)—in order to examine how a different arrangement of atoms in the target molecule is reflected in the TCS energy function. Similarities and differences of the TCS energy curves are pointed out and discussed.

A. 1-butyne, HC≡C–CH_2CH_3

Figure 1 shows the variation of the absolute TCS for a 1-butyne molecule measured in this work over the energy range from 0.3 to 300 eV. In addition, Fig. 1 includes our computations for 1-butyne: the integral ECS and ICS, as well as their sum, ECS + ICS, which represents the calculated overall cross section. The numerical values of the experimental TCS are listed in Table I, while Table II presents results of the ECS and ICS computations up to 3 keV. As no other absolute electron-scattering TCS data for 1-butyne, either experimental or theoretical, have been found in the literature, we also show in

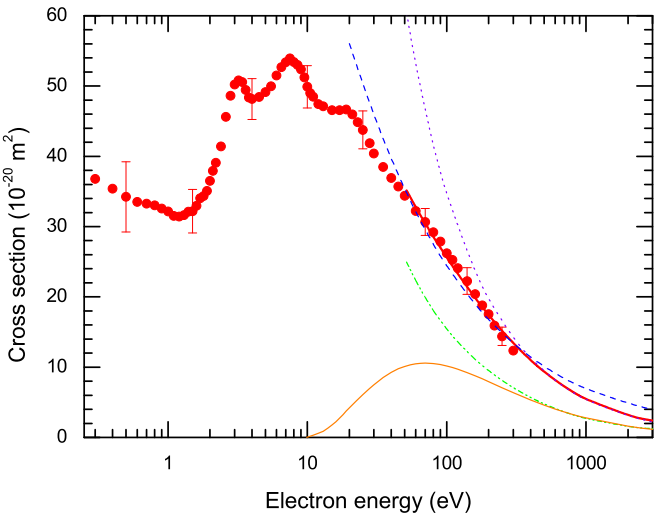

FIG. 1. (Color online) Cross sections for electron scattering from a 1-butyne molecule. Experimental: full (red) circles, TCS, present; error bars correspond to overall (systematic plus statistical) experimental uncertainties at selected points. Theoretical: dash-dot-dot (green) line, ECS calculated with the AR approach, present; thin-solid (orange) line, ICS in the BEB approximation, present; thick-solid (red) line, ECS + ICS, present. Empirical TCSs: dashed (blue) line, based on the formula from Ref. [30]; dotted (violet) line, using formula from Ref. [19].

Fig. 1 the empirical TCSs derived from the formulas developed by Floeder *et al.* [30] and Ariyasinghe and Villela [19], to compare and test their applicability.

The measured TCS energy dependence for the electron–1-butyne scattering, presented in Fig. 1, shows several distinct features. At the lowest applied electron-impact energies, below 1.2 eV, the TCS increases as the incident energy falls. This appearance of the TCS can be explained in terms of the direct long-range interaction between the impinging electron and a polar target molecule; a 1-butyne molecule has a moderate permanent electric dipole moment of about 0.7 D (cf. Table VI). In the vicinity of 1.2 eV, the TCS curve has a minimum of the value 31×10^{-20} m^2. Starting from about 1.5 eV, the TCS energy function rapidly increases, and at 3.2 eV it reaches its first local narrow maximum of about 51×10^{-20} m^2, followed by the minimum of 48×10^{-20} m^2 located around 4 eV. There is experimental evidence [8,9,14] that the 3.2 eV TCS peak can be related to the resonant processes. In the resonant scattering [57], the impinging electron of the appropriate energy is attached to the target molecule forming a temporary negative-ion state, which subsequently decays through the autodetachment of the extra electron, leaving the molecule in its vibrationally excited state and/or through the dissociation into negative and neutral fragments. The vibrational excitation of the electronic ground state of a 1-butyne molecule was observed in early experiments by Bowman and Miller [8] around 2.4 eV, while it was observed near 2.8 eV by Dance and Walker [9]. The formation of negative ions near 3.2 eV with an 8×10^{-24} m^2 yield was reported by Rutkowsky *et al.* [14].

Beyond the 4 eV minimum, the TCS shows a distinct hump spanned between 5 and 12 eV, peaking near 7.5 eV with a value of about 54×10^{-20} m^2. This broad TCS feature

TABLE I. Absolute experimental electron-scattering total cross sections (TCSs) for a 1-butyne molecule, in units of 10^{-20} m^2.

E (eV)	TCS	E (eV)	TCS	E (eV)	TCS	E (eV)	TCS	E (eV)	TCS
0.3	36.8								
0.4	35.4	1.8	34.4	4.5	48.4	12	47.4	60	32.2
0.5	34.2	1.9	35.1	5.0	49.2	13	47.1	70	30.7
0.6	33.5	2.0	36.5	5.5	50.0	15	46.6	80	29.2
0.7	33.3	2.1	37.9	6.0	51.5	17	46.6	90	27.9
0.8	33.0	2.2	39.1	6.5	52.7	19	46.7	100	26.2
0.9	32.6	2.4	41.4	7.0	53.4	21	46.0	110	25.3
1.0	32.2	2.6	45.6	7.5	53.9	23	44.9	120	24.1
1.1	31.5	2.8	48.6	8.0	53.4	26	43.8	140	22.2
1.2	31.4	3.0	50.2	8.5	53.0	28	41.9	160	20.4
1.3	31.6	3.2	50.8	9.0	52.4	30	40.4	180	18.8
1.4	32.1	3.4	50.6	9.5	51.2	35	38.5	200	17.6
1.5	32.2	3.6	49.5	10.0	49.9	40	36.9	220	15.9
1.6	33.0	3.8	48.4	10.5	49.0	45	35.7	250	14.4
1.7	34.0	4.0	48.2	11	48.5	50	34.4	300	12.4

closely resembles those observed for many other targets studied so far, as well as hydrocarbons. It seems to be well established that the appearance of the TCS maximum within 7–10 eV can be explained by the contribution from a number of weak inelastic components allowed at these energies, among them also resonant ones. In this electron-impact energy range, the electronic excitation [8,9] and direct dissociation [14] of 1-butyne were observed. From 20 eV upward, the TCS systematically decreases to about 12×10^{-20} m^2 near 300 eV, and it behaves with an energy like E^{-a}, where $a \sim 0.5$.

When considering Fig. 1 in more detail, one can discern some additional structures superimposed on the TCS curve. A weak shoulder visible around 0.8 eV might be associated with the resonant process; the formation of the negative fragment ion was observed at this energy [14]. Above the 8 eV maximum, a shoulder spanned between 12 and 26 eV is clearly visible; this TCS feature can be explained in terms of direct elastic and inelastic processes, which at these energies become relevant [8,9,14].

Regarding the computations, Fig. 1 shows that over the electron-impact energy range between 50 and 300 eV, the general energy dependence of the computed *total* cross section (sum of the integral ECS and ICS) for 1-butyne is similar to that of the experimental TCS. It is visible, however, that within 70 and 160 eV, the ECS + ICS results lie slightly below the measured TCS values, while above 180 eV the relationship reverses; the differences between calculated and measured cross sections do not exceed the experimental uncertainties. It is worth noting that below 30 eV, our ECS + ICS calculations (not shown here) significantly overestimate the experimental TCS values. That would be expected, as at such low energies the foundations of the additive rule approach used for the ECS calculations are not fulfilled completely.

Finally, we refer to the TCS curves in Fig. 1, which we generated for 1-butyne using the empirical formulas developed for hydrocarbons [19,30]. The empirical TCS curve, obtained using the formula of Floeder *et al.* [30], is in reasonable agreement with our experimental TCS and theoretical ECS + ICS results within 40–300 eV. At higher energies, beyond the experimental energy range, the empirical curve runs distinctly above the theoretical results. The TCS energy function, based on the empirical expression of Ariyasinghe and Villela [19], markedly overestimates the experimental TCS curve below 300 eV, while being in very good agreement with the theory at higher energies. A similar relationship between the experiment

TABLE II. Ionization (ICS) and elastic (ECS) cross sections calculated for electron impact on 1-butyne molecules; in units of 10^{-20} m^2.

E (eV)	ICS	E (eV)	ICS	ECS	E (eV)	ICS	ECS	E (eV)	ICS	ECS
9.913	0	25	6.10		85	10.5		350	5.80	6.20
10	0.023	30	7.50		90	10.4	16.6	400	5.33	5.67
11	0.304	35	8.53		95	10.3		450	4.93	5.17
12	0.593	40	9.26		100	10.2	15.4	500	4.59	4.76
13	0.880	45	9.77		110	9.95	14.4	600	4.04	4.11
14	1.318	50	10.1	25.6	120	9.72	13.6	700	3.62	3.62
15	1.78	55	10.3		140	9.24	12.2	800	3.28	3.23
16	2.24	60	10.5	22.3	160	8.77	11.1	900	3.00	2.93
17	2.75	65	10.6		180	8.34	10.2	1000	2.77	2.68
18	3.25	70	10.6	19.9	200	7.93	9.49	2000	1.60	1.52
19	3.74	75	10.6		250	7.07	8.08	2500	1.33	1.33
20	4.20	80	10.5	18.1	300	6.37	7.06	3000	1.14	1.25

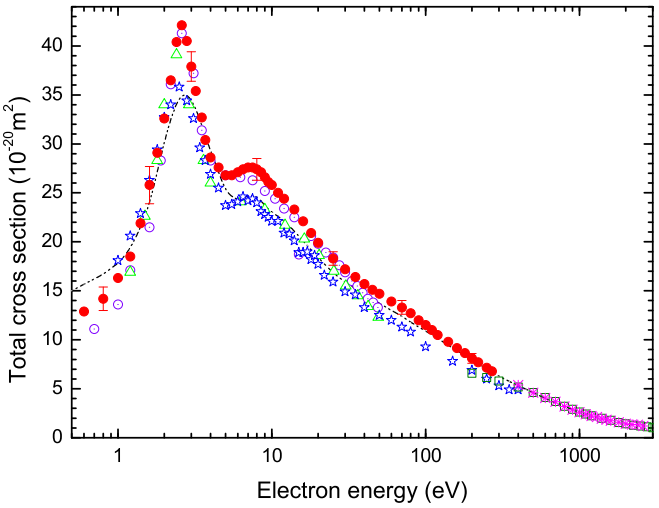

FIG. 2. (Color online) Total cross sections (TCSs) for electron scattering from an acetylene molecule. Experimental: full (red) circles, present absolute; error bars represent overall uncertainties; open (violet) circles, [15], absolute; open (green) triangles, [16], absolute; open (blue) stars, [21], normalized; (magenta) asterisks, [17], absolute; open (olive) squares, [19], absolute. Recommended: dash-dot-dot (black) line, [58].

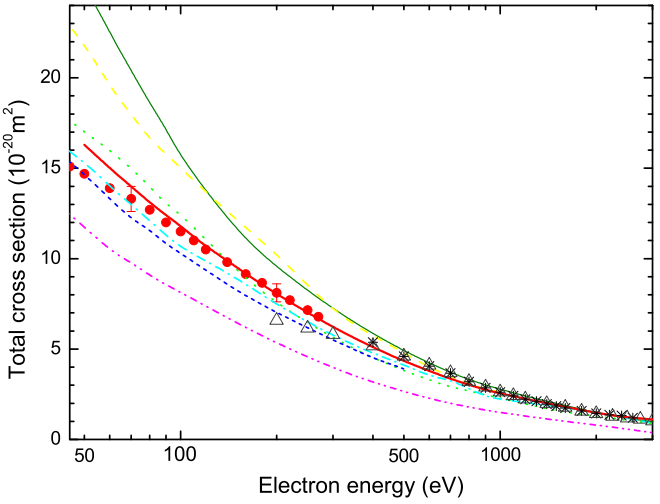

FIG. 3. (Color online) Total cross sections (TCSs) for electron scattering from an acetylene molecule. Experimental absolute: full (red) circles, present; error bars represent overall uncertainties; (black) asterisks, [17]; open (gray) triangles, [19]. Theoretical: thick-solid (red) line, ECS + ICS, present; thin-solid (olive) line, [22]; dashed (yellow) line, [23]; dotted (green) line, [24]; short-dash (blue) line, [25]; dash-dot (cyan) line, [27]; dash-dot-dot (magenta) line, [28].

and/or theory and the empirical curves based on these two formulas was noticed earlier (see, e.g., Ref. [41]), as well as for the other molecules of interest in the present work. This is what one would expect, keeping in mind that Floeder *et al.* [30] derived their formula based on experimental data between 100 and 400 eV, while Ariyasinghe and Villela [19] used measurements above 200 eV.

B. Acetylene, H–C≡C–H

The present experimental absolute TCS for acetylene, obtained in the 0.6–270 eV energy range, is shown in Fig. 2 and listed in Table III. In Fig. 2, we also show the TCSs measured earlier in several laboratories [15–17,19,21], together with the recommended TCS data [58] included for comparison. Between 50 and 200 eV, the present experimental results are the only absolute TCS data for acetylene obtained without any normalization procedure. In general, there is good agreement according to the shape of the experimental TCSs obtained by different experimental groups. All low-energy results shown in Fig. 2 reveal a prominent peak centered near 2.5 eV and a much broader weak hump located around 7.5 eV; both structures reflect the presence of resonances. However, some dispersion is visible in the magnitude of compared TCSs, especially at low and low-intermediate electron-impact energies. Our results are slightly higher in magnitude than those of the early measurements of Brüche [15] and Schmieder [16] in the overlapping energy range. More distinct, up to 10–20%, are discrepancies between the present absolute TCS data and normalized results of Sueoka and Mori [21]; the latter were commonly used as the reference standard for calculations. Also, the TCS values of Ariyasinghe and Villela [19] at 200 and 250 eV are lower than the present measurements by about 15%.

Figure 3 shows the present ECS + ICS calculations over the energy range from 50 to 3000 eV, which are compared with the present experimental absolute TCSs at intermediates and those

TABLE III. Absolute experimental electron-scattering total cross sections for an acetylene molecule, in units of 10^{-20} m^2.

E (eV)	TCS	E (eV)	TCS	E (eV)	TCS	E (eV)	TCS	E (eV)	TCS
0.6	12,9	2.8	40.5	7.0	27.6	18	20.9	90	12.0
0.8	14.2	3.0	37.9	7.5	27.6	20	19.9	100	11.5
1.0	16.3	3.2	35.4	8.0	27.4	25	18.3	110	11.0
1.2	18.5	3.5	32.7	8.5	27.1	30	17.2	120	10.5
1.4	21.9	3.7	30.4	9.0	26.6	35	16.4	140	9.81
1.6	25.8	4.0	28.6	9.5	26.1	40	15.7	160	9.15
1.8	29.1	4.5	27.6	10	25.8	45	15.1	180	8.66
2.0	32.6	5.0	26.8	11	25.0	50	14.7	200	8.11
2.2	36.5	5.5	26.8	12	24.4	60	13.9	220	7.71
2.4	40.4	6.0	27.1	14	23.3	70	13.3	250	7.15
2.6	42.1	6.5	27.4	16	22.1	80	12.7	270	6.79

TABLE IV. Ionization and elastic cross sections calculated for electron impact on acetylene molecules, in units of 10^{-20} m^2.

E (eV)	ICS	E (eV)	ICS	ECS	E (eV)	ICS	ECS	E (eV)	ICS	ECS
11.122	0	25	2.73		100	4.55	7.23	450	2.208	2.478
12	0.191	27.5	3.06		110	4.45	6.78	500	2.057	2.281
13	0.417	30	3.35		120	4.34	6.39	600	1.811	1.971
14	0.640	35	3.81		140	4.13	5.75	700	1.621	1.737
15	0.853	40	4.14		160	3.92	5.25	800	1.469	1.555
16	1.054	45	4.37		180	3.73	4.84	900	1.345	1.408
17	1.242	50	4.52	11.8	200	3.55	4.50	1000	1.241	1.288
18	1.450	60	4.68	10.3	250	3.16	3.84	2000	0.716	0.729
19	1.646	70	4.73	9.25	300	2.85	3.37	2500	0.596	0.632
20	1.856	80	4.70	8.42	350	2.60	3.00	3000	0.512	0.590
22.5	2.327	90	4.64	7.77	400	2.39	2.71			

of Xing *et al.* [17] and Ariyasinghe and Villela [19] at high electron-impact energies. Numerical values of our ECS and ICS are listed in Table IV. The TCS results of the previous theoretical investigations for electron-acetylene scattering reported in the literature [22–25,27,28] are also shown in Fig. 3. It is clearly seen that particular theoretical TCSs in the range 30–3000 eV differ significantly in magnitude, even by a factor of 2. Generally, the earlier computations reproduce the experimental findings mainly qualitatively. Only the calculations of Joshipura and Vinodkumar [24] and Shi *et al.* [27] do not differ from experiments by more than 16% and 12%, respectively. Figure 3 shows that our calculated ECS + ICS values are in very close agreement with the experimental TCS data ranging from about 80 eV up to 3 keV; differences do not exceed 6%.

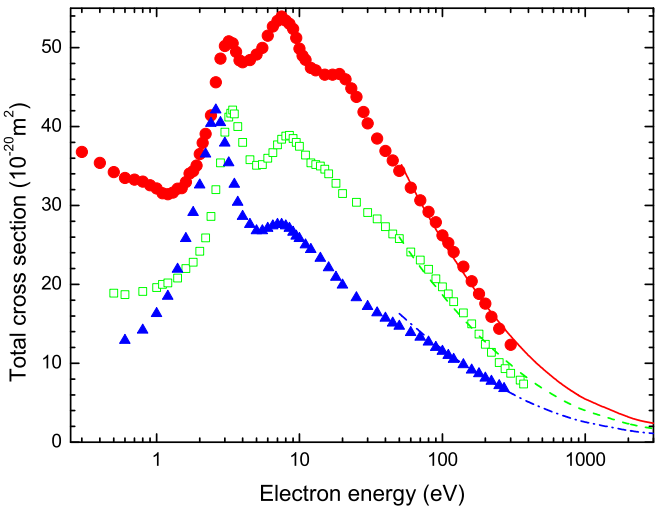

FIG. 4. (Color online) Comparison of total absolute cross sections for electron scattering from the acetylene molecule and its derivatives, measured (TCSs) and calculated (ECS + ICS) in our laboratory. HC≡C–H: full (blue) triangles, present experiment; dash-dot (blue) line, present calculations. HC≡C–CH_3: open (green) squares, experiment [31]; dashed (green) line, present computations. HC≡C–CH_2CH_3: full (red) circles, present measurements; solid (red) line, present calculations.

C. Comparison of TCSs for electron scattering from structurally related alkynes: Acetylene (HC≡CH), propyne (HC≡C–CH_3), and 1-butyne (HC≡C–CH_2CH_3)

In this section, we examine how the replacement of one hydrogen atom in the acetylene molecule with a given group of atoms is reflected in the TCS energy dependence. For this purpose, in Fig. 4 we compare our experimental and theoretical TCSs for acetylene with those for its substituted homologues: propyne and 1-butyne. As the calculations of the electron-propyne scattering cross sections at energies above 50 eV are not available in the literature, we listed our computed ECS and ICS (the main components of the TCS) values in Table V, up to 3000 eV. Each member of the examined alkyne family has, on one of the ends of the molecule chain, the triple carbon-to-carbon bond. In subsequent molecules of the family, one hydrogen atom in the acetylene molecule is replaced with the methyl group (CH_3) to form a propyne molecule (HC≡C–CH_3) or with the ethyl group (CH_2CH_3) to form 1-butyne (HC≡C–CH_2CH_3). The schematic geometry of the considered compounds is shown in Fig. 5.

Referring to Fig. 4, one can see that, according to the shape, the TCS for 1-butyne generally resembles that for acetylene and for propyne. All compared TCS energy functions have the distinct asymmetric enhancement with two maxima: the first maximum is located within 2.4–3.5 eV, and the second one is between 6 and 9 eV. The first, narrow TCS maximum in each curve is related to the electron-molecule scattering proceeding with the formation of the temporary negative-ion state. This resonant maximum shifts slightly in energy, from 2.6 eV to 3.4 and 3.2 eV, respectively, while going from acetylene to propyne and 1-butyne. It is evident that the intensity of the lowest TCS peak with respect to the TCS background decreases with the increasing size of the functional unit replacing one hydrogen atom in the acetylene molecule. As shown in Fig. 4, the second

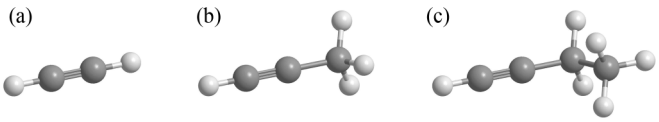

FIG. 5. Schematic geometry of (a) the acetylene (HC≡C–H) molecule and its substituted derivatives: (b) propyne (HC≡C–CH_3) and (c) 1-butyne (HC≡C–CH_2CH_3).

TABLE V. Ionization and elastic cross sections calculated for electron impact on propyne molecules, in units of 10^{-20} m^2.

E (eV)	ICS	E (eV)	ICS	ECS	E (eV)	ICS	ECS	E (eV)	ICS	ECS
10.216	0	22.5	3.78		90	7.48	12.2	400	3.836	4.194
11	0.207	25	4.41		100	7.34	11.3	450	3.549	3.826
12	0.482	27.5	4.95		110	7.18	10.6	500	3.305	3.520
13	0.754	30	5.42		120	7.01	9.99	600	2.909	3.038
14	1.012	35	6.17		140	6.66	8.98	700	2.603	2.676
15	1.254	40	6.69		160	6.32	8.18	800	2.359	2.394
16	1.611	45	7.06		180	6.01	7.53	900	2.159	2.167
17	1.974	50	7.31	18.7	200	5.72	7.00	1000	1.992	1.982
18	2.327	60	7.57	16.3	250	5.09	5.96	2000	1.148	1.125
19	2.685	70	7.64	14.6	300	4.59	5.21	2500	0.956	0.980
20	3.023	80	7.59	13.2	350	4.18	4.64	3000	0.821	0.922

TCS maxima for the acetylenic family are centered near the same energy: around 7.5 eV for acetylene, close to 8.5 eV for propyne, and again near 7.5 eV for 1-butyne. Such behavior is similar to that for a series of alkanes, for which the location of the main maximum practically does not change [59], but it differs from the alkenes family [41].

The substitution of one hydrogen atom in the acetylene molecule with a functional unit of increasing length enlarges the size of the resulting compound and, as a consequence, should lead to the increase of the respective electron-scattering TCS values. However, it is apparent from Fig. 4 that according to the magnitude of the TCS, one can distinguish three energy regions. Below 1.5 eV, the observed trend in the magnitude of TCSs across the series of target molecules rather confirms the expected increase of TCS values with the size of the substituent unit. Between 1.5 and 4 eV, where the resonant effects considerably influence the scattering process, the electron-molecule interaction becomes more sensitive to the structure of the target molecule than to its size. Above 5 eV, the compared TCS curves behave very similarly with respect to the shape, and the magnitude of the TCS generally increases across the investigated series of molecules. It is interesting that above the ionization threshold, the increment of the TCS, due to the replacement of one hydrogen atom with the ethyl (CH_2CH_3) group, is nearly twice that due to the methyl unit (CH_3). A similar *substitutional* trend in the TCS magnitude was already observed for molecules of the alkene (C_nH_{2n}) series [41].

Further inspection of Fig. 4 reveals that the ratio of the intensity of the low-energy structure (within 2–4 eV) to the intensity of the next TCS maximum (located between 6 and 9 eV) drastically decreases across the acetylenic derivatives with the enlargement of the substituent group, in contrast to the ethylenic series [41]. While for acetylene the amplitude of the first TCS peak above the TCS background is nearly ten times higher than the second one, for propyne this ratio falls to about two, and for 1-butyne both TCS features exceed the background to a similar degree. Such TCS behavior might be due to the different charge redistribution on the site of the H–C≡C unit across a class of homologous compounds, and, as a consequence, different interaction between the substituent group orbitals and the orbitals of this acetylenic unit.

Beyond 10 eV, an additional feature in the TCS curves is perceptible, and its intensity becomes more and more distinct when going from acetylene to 1-butyne. While for acetylene a weak change in the TCS slope is barely distinguishable near 15 eV, for propyne a weak shoulder within 13–18 eV is rather noticeable, being a pronounced shoulder centered near 19 eV for 1-butyne. A similar behavior of TCS curves in the energy region just beyond the main TCS maximum was already observed for both a series of alkanes [59] and alkenes [41].

Finally, Fig. 4 shows that our calculations for propyne reasonably reproduce the experimental TCS, similarly to the two remaining molecules, which is why we believe the computed ECS + ICS values correctly predict the TCS for the propyne molecule also above the experimental energy range.

D. Comparison of the electron scattering TCSs for isomers of the C_4H_6 molecule: 1-butyne, 2-butyne, and 1,3-butadiene

Having in hand the experimental absolute TCS data for some C_4H_6 compounds, we can examine how a different arrangement of atomic components of molecule influences the electron-scattering cross sections. In Fig. 6, we

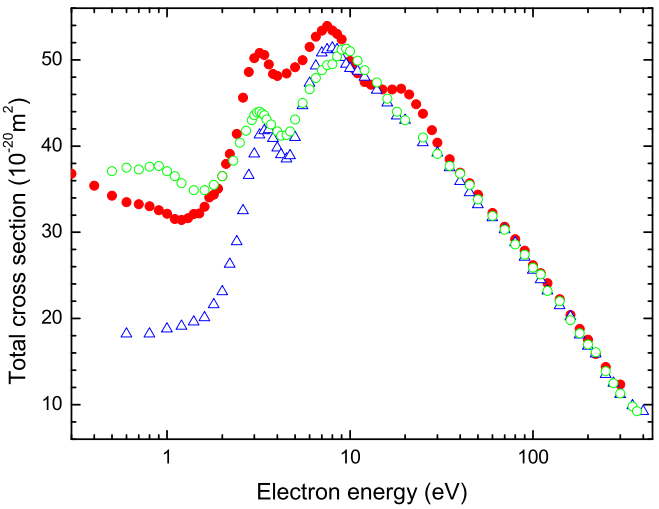

FIG. 6. (Color online) Comparison of total absolute cross sections measured in our laboratory for electron scattering from C_4H_6 isomers: HC≡C–CH_2CH_3, full (red) circles, present; H_3C–C≡C–CH_3, open (blue) triangles, [32]; H_2C=CHCH=CH_2, open (green) circles, [32].

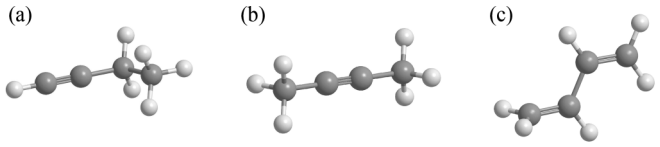

FIG. 7. Schematic geometry of C_4H_6 isomers: (a) 1-butyne ($HC{\equiv}C–CH_2$-CH_3); (b) 2-butyne ($H_3C–C{\equiv}C–CH_3$), and (c) 1,3-butadiene ($H_2C{=}CHCH{=}CH_2$) molecules.

compare the absolute TCSs measured for 1-butyne ($HC{\equiv}C–CH_2CH_3$), 2-butyne ($H_3C–C{\equiv}C–CH_3$), and 1,3 butadiene ($H_2C{=}CHCH{=}CH_2$), the straight-chained isomers of the C_4H_6 compound. Figure 7 shows the geometric structures of the considered C_4H_6 isomers.

1-butyne and 2-butyne have one carbon-to-carbon triple bond, whereas 1,3 butadiene is a compound with conjugated double carbon-carbon bonds. A different arrangement of atoms in isomers leads to a different distribution of the electric charge in molecules (cf. Table VI). As the *isomeric effect* for 2-butyne and 1,3-butadiene molecules has already been discussed [32,60], only a brief outline of the general features in the TCS energy functions is given here, and some other observations are pointed out.

Figure 6 clearly shows that below the ionization threshold, where resonant processes distinctly contribute to the scattering, the shape and magnitude of TCS energy functions are sensitive to the arrangement of constituent atoms in the molecule. At such low energies, the impinging electron does not penetrate the molecule too much, rather it sees the molecule as a whole. Therefore, the electron-molecule interaction is determined by the molecular character of the target, and the distribution of the electric charge in the molecule—expressed by the permanent electric dipole moment and dynamic target polarization (see Table VI)—plays an essential role in the scattering. The TCS values obey the following relations: below 2 eV, TCS(1,3-butadiene) > TCS(1-butyne) > TCS(2-butyne); between 2 and 5.5 eV, TCS(1-butyne) > TCS(1,3-butadiene) > TCS(2-butyne); while around the main maximum, TCS(1-butyne) > TCS(2-butyne) > TCS(1,3-butadiene). The interesting TCS difference is also noticeable around 20 eV, where the TCS for 1-butyne has a distinct shoulder—a feature not perceptible for the other members of the isomeric series. In this energy range, the TCS magnitude for 1-butyne distinctly exceeds those for 2-butyne and 1,3-butadiene.

TABLE VI. Selected electric parameters of considered compounds (from Ref. [61]): permanent dipole moment, μ, and dipole polarizability, α: for 2-butyne, the α value was estimated using the additivity method [62].

Molecule	μ (Debye)	α (10^{-30} m^3)
$HC{\equiv}CH$; acetylene	0	3.33
$HC{\equiv}C–CH_3$; propyne	0.784	6.18
$HC{\equiv}C–CH_2CH_3$; 1-butyne	0.782	7.41
$H_3C–C{\equiv}C–CH_3$; 2-butyne	0	7.2
$H_2C{=}CHCH{=}CH_2$; 1,3-butadiene	0	8.64

Above 30 eV, the magnitude of TCS for examined isomers is practically the same. Such TCS behavior seems to indicate that at higher impact energies, the interaction of the impinging electron with the constituent atoms is more adequate for the description of the electron-molecule collision and justifies the application of the independent atom approximation for TCS calculations at intermediate and high electron impact energies.

V. SUMMARY

In the present paper, we report on the experimental and theoretical electron-impact cross sections for simple open-chain hydrocarbons. Absolute total cross sections (TCSs) for 1-butyne and acetylene molecules have been measured at impact energies from low to intermediate. The TCS energy function for 1-butyne exhibits a low-energy resonant maximum located near 3.2 eV, the broader hump peaking around 7.5 eV, and the shoulder between 12 and 26 eV; beyond 30 eV, the TCS decreases continuously. We found a close agreement in the shape of the present measured TCS curve for acetylene with the earlier TCSs available in the literature, although the present data are generally larger in magnitude. Our absolute TCSs for acetylene are between 50 and 200 eV, the only measured TCS obtained without a normalization procedure. These results would be useful when preparing recommended data.

The sum, ECS + ICS, of our calculated elastic (ECS) and ionization (ICS) cross sections reproduces reasonably the experimental TCS data above 50 eV for the acetylenic family: acetylene ($HC{\equiv}CH$), propyne ($HC{\equiv}C–CH_3$), and 1-butyne ($HC{\equiv}C–CH_2CH_3$). The consistency of the experimental and theoretical data allows us to expect that also beyond the energy range of the present TCS experiment, i.e., above 300 eV, the calculated ECS + ICS values represent the TCS for 1-butyne and propyne satisfactorily.

We observed a close similarity in the shape of the experimental TCS curves for an acetylene molecule and its derivatives: propyne and 1-butyne. Generally, the magnitude of the TCS for this series of alkynes increases with the enlargement of the molecular target size. Finally, the structural effect is indicated in the TCS energy functions for three isomers of the C_4H_6 compound: 1-butyne ($HC{\equiv}C–CH_2CH_3$), 2-butyne ($H_3C–C{\equiv}C–CH_3$), and 1,3-butadiene ($H_2C{=}CHCH{=}CH_2$). The differences in the arrangement of atoms across the considered series of molecules lead to differences in the shape and magnitude of TCSs at low impact energies, where resonant scattering processes are important, while at impact energies higher than 50 eV, where direct processes dominate the scattering, the TCS curves for isomers practically coincide.

ACKNOWLEDGMENTS

This work has been partially supported by the Polish Ministry of Science and Higher Education (MNiSzW Project 2013-2014). Numerical calculations have been performed at the Academic Computer Center (TASK) in Gdańsk.

[1] L. Sanche, Eur. Phys. J. D **35**, 367 (2005).
[2] D. Field, Europhys. News **36**, 51 (2005).
[3] L. G. Christophorou and J. K. Olthoff, *Fundamental Electron Interactions with Plasma Processing Gases* (Kluwer Academic, New York, 2004).
[4] Y. Itikawa, *Molecular Processes in Plasmas* (Springer, Berlin, 2007).
[5] E. Böhler, J. Warneke, and P. Swiderek, Chem. Soc. Rev. **42**, 9219 (2013).
[6] F. H. Coats and R. C. Anderson, J. Am. Chem. Soc. **79**, 1340 (1957).
[7] J. Collin and F. P. Lossing, J. Am. Chem. Soc. **79**, 5848 (1957).
[8] C. R. Bowman and W. D. Miller, J. Chem. Phys. **42**, 681 (1965).
[9] D. F. Dance and I. C. Walker, J. Chem. Soc. Faraday Trans. II **70**, 1426 (1974).
[10] R. S. Stradling, M. A. Baldwin, A. G. Loudon, and A. Maccoll, J. Chem. Soc. Faraday Trans. II **72**, 871 (1976).
[11] W. M. Flicker, O. A. Mosher, and A. Kuppermann, J. Chem. Phys. **69**, 3311 (1978).
[12] A. Kuppermann, W. M. Flicker, and O. A. Mosher, Chem. Rev. **79**, 77 (1979).
[13] O. Bastiansen, P. Bakken, E. Kloster-Jensen, S. Samdal, and M. Trætteberg, J. Mol. Struct. **352-353**, 77 (1995).
[14] J. Rutkowsky, H. Drost, and H.-J. Spangenberg, Ann. Phys. (Leipzig) **492**, 259 (1980).
[15] E. Brüche, Ann. Phys. (Leipzig) **394**, 909 (1929).
[16] F. Schmieder, Z. Elektrochem. Angew. Phys. Chem. **36**, 700 (1930).
[17] S. L. Xing, Q. C. Shi, X. J. Chen, K. Z. Xu, B. X. Yang, S. L. Wu, and R. F. Feng, Phys. Rev. A **51**, 414 (1995).
[18] W. M. Ariyasinghe and D. Powers, Phys. Rev. A **66**, 052716 (2002).
[19] W. M. Ariyasinghe and G. Villela, Nucl. Instrum. Methods Phys. Res. B **268**, 2217 (2010).
[20] R. Dressler and M. Allan, J. Chem. Phys. **87**, 4510 (1987).
[21] O. Sueoka and S. Mori, J. Phys. B **22**, 963 (1989).
[22] A. Jain and K. L. Baluja, Phys. Rev. A **45**, 202 (1992).
[23] Y. Jiang, J. Sun, and L. Wan, Z. Phys. D **34**, 29 (1995).
[24] K. N. Joshipura and M. Vinodkumar, Eur. Phys. J. D **5**, 229 (1999).
[25] I. Iga, M.-T. Lee, P. Rawat, L. M. Brescansin, and L. E. Machado, Eur. Phys. J. D **31**, 45 (2004).
[26] M. Vinodkumar, K. N. Joshipura, C. G. Limbachiya, and B. K. Antony, Eur. Phys. J. D **37**, 67 (2006).
[27] D. Shi, Y. Liu, J. Sun, H. Ma, and Z. Zhu, Rad. Phys. Chem. **77**, 528 (2008).
[28] M. Vinodkumar, A. Barot, and B. Antony, J. Chem. Phys. **136**, 184308 (2012).
[29] G. G. Raju, *Gaseous Electronics: Tables, Atoms, and Molecules* (CRC, Boca Raton, FL, 2011).
[30] K. Floeder, D. Fromme, W. Raith, A. Schwab, and G. Sinapius, J. Phys. B **18**, 3347 (1985).
[31] Cz. Szmytkowski and S. Kwitnewski, J. Phys. B **35**, 3781 (2002).
[32] Cz. Szmytkowski and S. Kwitnewski, J. Phys. B **36**, 2129 (2003).
[33] Cz. Szmytkowski, P. Możejko, and G. Kasperski, J. Phys. B **30**, 4363 (1997); Cz. Szmytkowski and P. Możejko, Vacuum **63**, 549 (2001); A. Domaracka, P. Możejko, E. Ptasińska-Denga, and Cz. Szmytkowski, J. Phys. B **39**, 4289 (2006).
[34] M. Knudsen, Ann. Phys. (Leipzig) **31**, 205 (1910).
[35] M. A. Khakoo, J. Muse, C. Campbell, M. C. A. Lopes, H. Silva, C. Winstead, and V. McKoy, J. Phys.: Conf. Ser. **194**, 012027 (2009).
[36] B. Bederson and L. J. Kieffer, Rev. Mod. Phys. **43**, 601 (1971).
[37] J. P. Sullivan, J. Makochekanva, A. Jones, P. Caradonna, D. S. Slaughter, J. Machacek, R. P. McEachran, D. W. Mueller, and S. J. Buckman, J. Phys. B **44**, 035201 (2011).
[38] R. N. Nelson and S. O. Colgate, Phys. Rev. A **8**, 3045 (1973).
[39] Cz. Szmytkowski, P. Możejko, E. Ptasińska-Denga, and A. Sabisz, Phys. Rev. A **82**, 032701 (2010).
[40] P. Możejko, E. Ptasińska-Denga, and Cz. Szmytkowski, Eur. Phys. J. D **66**, 44 (2012).
[41] Cz. Szmytkowski, P. Możejko, M. Zawadzki, and E. Ptasińska-Denga, J. Phys. B **46**, 065203 (2013).
[42] N. F. Mott and H. S. W. Massey, *The Theory of Atomic Collisions* (Oxford University Press, Oxford, 1965).
[43] D. Raj, Phys. Lett. A **160**, 571 (1991).
[44] Y.-K. Kim and M. E. Rudd, Phys. Rev. A **50**, 3954 (1994).
[45] W. Hwang, Y.-K. Kim, and M. E. Rudd, J. Chem. Phys. **104**, 2956 (1996).
[46] P. Możejko, B. Żywicka-Możejko, and Cz. Szmytkowski, Nucl. Instrum. Methods Phys. Res. B **196**, 245 (2002).
[47] P. Możejko and L. Sanche, Radiat. Environ. Biophys. **42**, 201 (2003).
[48] F. Salvat, J. D. Martinez, R. Mayol, and J. Parellada, Phys. Rev. A **36**, 467 (1987).
[49] N. T. Padial and D. W. Norcross, Phys. Rev. A **29**, 1742 (1984).
[50] J. P. Perdew and A. Zunger, Phys. Rev. B **23**, 5048 (1981).
[51] X. Zhang, J. Sun, and Y. Liu, J. Phys. B **25**, 1893 (1992).
[52] M. J. Frisch *et al.*, GAUSSIAN 03, *Revision B.05* (Gaussian, Pittsburgh, 2003).
[53] W. von Niessen, J. Schirmer, and L. S. Cederbaum, Comput. Phys. Rep. **1**, 57 (1984).
[54] J. V. Ortiz, J. Chem. Phys. **89**, 6348 (1988).
[55] L. S. Cederbaum, J. Phys. B **8**, 290 (1975).
[56] V. G. Zakrzewski and W. von Niessen, J. Comput. Chem. **14**, 13 (1994).
[57] K. Takayanagi, in *Electron-Molecule Collisions*, edited by I. Shimamura and K. Takayanagi (Plenum, New York, 1984).
[58] *Photon and Electron Interactions with Atoms, Molecules and Ions*, edited by Y. Itikawa, Landoldt-Börnstein Vols. 17A–C (Springer, Berlin, 2000–2003).
[59] O. Sueoka, C. Makochekanwa, H. Tanino, and M. Kimura, Phys. Rev. A **72**, 042705 (2005).
[60] A. R. Lopes, M. A. P. Lima, L. G. Ferreira, and M. H. F. Bettega, Phys. Rev. A **69**, 014702 (2004).
[61] *Handbook of Chemistry and Physics*, 76th ed., edited by D. R. Lide (CRC, Boca Raton, FL, 1995–1996).
[62] K. J. Miller, J. Am. Chem. Soc. **112**, 8533 (1990).